A Short Review of 2D-Discrete Dislocation Modeling for Fracture/Fatigue

Olarnrithinun S.

Metal Deformation Technology Laboratory, National Metal and Materials Technology Center
114 Thailand Science Park, Paholyothin Rd, Klong1, Klong Luang, Pathumthani., Thailand
E-mail address: suteeo@mtec.or.th

Abstract

The discrete dislocation (DD) plasticity is truly mechanism-based plasticity and well-suited for mesoscale modeling in metal. The effects of size-dependent plasticity and plastic dissipation emerge naturally from this framework. The micromechanics of fracture are material dependent and involve a broad range of length and time scales. The intermediate situation between the cleavage crack growth and the plastic dissipation involved in fracture based on DD plasticity is focused here. Fracture crack growth is affected by dislocations: (i) dislocation motion shields the crack tip and increases the dissipation energy and (ii) the local stress concentration associated with discrete dislocation in the vicinity of the crack tip can reach atomic bond strength, causing the crack to grow. In this paper a few problems of fracture, such as fatigue crack growth from small cracked particle into single crystal and the role of plastic anisotropy on crack growth in a single crystal, are reviewed with a focus on the effects of plastic confinement around a crack tip.

Keywords*: Fatigue, Fracture, Multiscale Modeling, Discrete Dislocation, Finite Element Method*

1 Introduction

Fracture is the process of separating a solid object into two or more pieces and then the new surface inside the object is created. Generally, this involves nucleation and propagation of crack-like defects. In most fields, growth is much better understood than crack nucleation since the crack nucleation is more complicated. That is why most fracture studies have been focused on growth initiation and propagation of pre-existing crack. A key difficulty is that fracture spans several length scales from the atomistic scale to the macroscopic scale, in Figure 1.

Figure 1 shows the important length scales involved for cleavage crack growth in ductile materials. At the sufficiently large scale as shown in Figure 1 (a), stress and deformation fields near a crack tip can be described in terms of a macroscopic and often isotropic model that continuum methods are employed. Under small scale yielding where the plastic flow and separation region are very small compared to the crack length, the stress intensity factor (K) in linear elastic fracture mechanics (LEFM) serves as characterizing parameter to describe the near crack tip stress field, while the energy release rate is used as characterizing parameter when the plastic flow becomes larger compared to the crack length. The conventional continuum plasticity can significantly reduce the number of degrees of freedom relative to atomic simulations and then incorporation of a material length scale is also necessary to capture the defect behaviors, i.e. shear bands and strain localization. Such defect behaviors are subsumed into effective constitutive laws for the material deformation by introducing a material parameter with the dimensions of length. The continuum model of fracture processes containing a length scale has been developed [1-3]. Despite the substantial successes, the material length scale over the continuum description is not straightforward due to the requirement from experimental data for the prediction.

At the smaller scale in Figure 1 (b), the anisotropic nature of individual grains comes into play. The fluctuation of stress and strain can be described by crystal plasticity modeling which is one of mesoscale frameworks. Over last two decades, computational studies of crystal plasticity have made major contributions to understand the mechanical behavior of materials [4-8]. One main advantage of crystal plasticity models incorporating Finite Element Method (FEM) lies in capability to solve crystal

mechanical problems under complicated internal and/or external boundary condition. It is an inherent part of the physics of crystal mechanics dealing with the delicate interplay of different effects, not only the complicated boundary but also various deformation mechanisms, the dislocation mean free path or the characteristic length scale of crystal plasticity and their interactions, such as dislocation slip, twinning and a martensitic transformation, implemented through the constitutive relations.

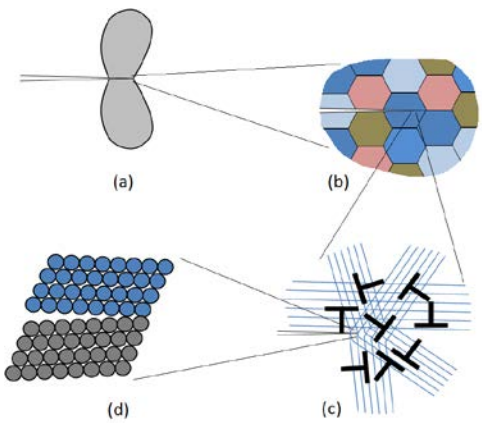

Figure 1: The various relevant scales in fracture: (a) the macroscopic scale that the plastic zone is governed by continuum plastic flow (b) the grain scale in a polycrystalline metal (c) the scale of discrete dislocations and of discrete slip planes (d) the atomic scale.

Closer to the crack tip in the single crystal, Figure 1 (c), the energy dissipation, associated with the mobile dislocations moving through the lattice, and effective material separation laws (cohesive zones) of crack nucleation and growth dominate on this mesoscale. There is lots of experimental evidence at this mesoscale showing the size dependence effect of plastic flow; smaller is stronger. Also the fracture processes are composed of the underlying physical mechanisms of both irreversible deformation (i.e. plastic dissipation) and material separation (i.e. atomic bond breaking). The importance of failure mechanisms, such as nucleation, growth and coalescence of voids or fracture, and interaction between defects, occurs on this mesoscale modeling of which the formulations are intermediate between an atomistic and an unstructured continuum description, or crystal plasticity, of deformation processes. Descriptions of such phenomena thus rely on simplified model of the defects, where atomistic details such as the core structure of a dislocation are neglected. Alternative method to eliminate the atomistic degree of freedom and to consider only the tracking explicit defects is discrete dislocation dynamics [9-17]. The discrete dislocation modeling solves boundary value problems for the body containing dislocations which are characterized entirely by continuum representations using concepts such as eigenstrains and introducing mobility laws to capture the motion of the dislocations under applied stresses. Discrete dislocation plasticity has emerged as a mean to study plastic deformation, providing fundamental understanding of hardening/strengthening, size effects and plastic dissipation naturally. This framework does not require the specification of elastic-plastic constitutive laws. The length scale of this approach can be varied and depends on a spacing of obstacles resulting in slip band spacing or dislocation pileups, more detail in section 2.

As shown in Figure 1 (d), the actual separation process takes place at the atomic scale. The stress fields from the next higher-up scales increase the stress level of the atomic bonds to be broken when the stresses at this scale reach the value on the order of bond strength. Atomistic models certainly incorporate the proper underlying mechanics, but they are not practical for the analysis of larger mesoscale structure. However atomistic simulations are particularly useful for investigating the interaction of defects and structural evolution, such as during deposition of atoms onto a surface, including finite temperature behavior and motion of defects and atoms [18-21]. Such simulations provide insight into the fundamental behavior and provide information that can be passed to larger-scale models. Atomistic methods follow the motion of the ion as atom interaction via effective classical interatomic potentials. A form in widespread use for metallic systems is the embedded-atom method (EAM) [22-24] potential where parameters are varied to fit a wide range of material properties as obtained by either experiment or quantum calculations. A typical set of properties used in the fit are equilibrium lattice structure and lattice constants, elastic moduli, surface energies and vacancy formation energy. Hence, quantum methods are useful for determining crystal structure and elastic constants as well as capturing the chemistry of alloying and some details of individual defects such as vacancies and dislocations. It is worth noting that as a general rule, computations on smaller

size scales require smaller time steps. Computational power limits such studies to millions of atoms, typically, corresponding to submicron volumes of material. In materials that deform plastically and/or undergo fatigue degradation, the collective behavior of defects, especially dislocations, occurs on much larger scales of microns to millimeters.

The above mention emphasized the fact that fracture is highly localized at the atomic scale but is driven by the macroscopic applied load to atomic scale via stress field on smaller length scales. Here, we briefly review some aspects of modeling in mesoscale where dislocation plays a key role in mediating between atomic scale effect and dissipation process via discrete dislocation modeling to fracture problems. In this paper the analysis of fatigue crack growth from micron-scale particle and the role of plastic anisotropy for the basal cleavage in HCP-like materials are reviewed. Finally the limitation of this framework and prospects for future improvement will be discussed.

2 Discrete dislocation plasticity

Discrete dislocation (DD) method has been applied to study plastic deformation at sub-continuum scales over the last two decades, providing understanding of strengthening/hardening phenomena and of size effects in plasticity [9, 25-33]. The DD method solves boundary value problems for isotropic elastic bodies which contain mobile dislocations. Without any special constitutive model, plastic deformation is described through the motion of large number of discrete dislocations, which are treated as singularities in an isotropic elastic solid. The DD method is well-suited for micro-scale deformation analysis in metals since size-dependent plastic flow emerges naturally from strain/stress gradients through the discrete dislocation evolution. With only a few physically-based constitutive rules governing the short range dislocation interactions (e.g. dislocation nucleation, motion and annihilation), the DD method has shown a remarkable ability to reproduce complicated physical phenomena such as fatigue crack [28-30, 34]; a strong Bauschinger effect during unloading of a metal matrix composite with elastic particle reinforcements [35]; and that the Mode-I crack tip fields in a single crystal are in good agreement with analytical crystal plasticity solution [36,37].

This section briefly presents an overview of the standard DD methodology by Van der Giessen and Needleman (1995) [9] and its numerical implementation for a crack problem. The DD method plays a dual role in fracture; (i) their motion leading to plastic flow increases the resistance to crack growth; (ii) the crack propagation is promoted by the local stress concentration associated with the dislocations. Each dislocation induces a localized stress concentration, giving rise to large local stress fluctuations that vary as dislocations moving. The dislocations can also be generated from nearby sources. Special attention is given to aspects of the formulation that, for computational reasons, tend to discourage its application to problems with instability in dislocation velocity, elastic inhomogeneities and difficulties in capturing micrometer of crack growth with sub-angstrom mesh sizes around the crack tip. These limitations are avoided using a new algorithm for discrete dislocation modeling of fracture proposed by [39-41].

2.1 *A general framework*

The two dimensional plane strain DD (2d-DD) method has been widely used to provide insight into a variety of fracture problems [9]. Attention is focussed on small strain and small scale yielding for crack tip plasticity. Thus the stress intensity factor (K) is used to characterize the loading type of fracture. The discrete dislocation framework models dislocations as point defects in an isotropic elastic material where they glide on a discrete set of slip planes. The edge dislocation lines are straight and parallel to the out of plane direction. Long range dislocation interactions operate through their singular continuum elastic fields. These fields are expected to accurately characterize the dislocation beyond distances of several times the Burgers vector from the dislocation core [42]. Short range dislocation interactions are governed by a set of constitutive rules for dislocation nucleation, motion, and annihilation, which were proposed by [43]. These rules are designed to approximate the complicated atomic-level interactions of dislocation segments that approach within a few Burgers vectors. In fact realistic dislocation interactions are more complex and so rules for junction formation and destruction, dislocation climb, and cross slip also exist. In 2d-DD, dislocation nucleation is assumed as the creation of a dislocation dipole to mimic the mechanism of Frank-Read loop expansion. The dislocation segment glides with a velocity which is proportional to the Peach-Koehler force resolved on the dislocation segment.

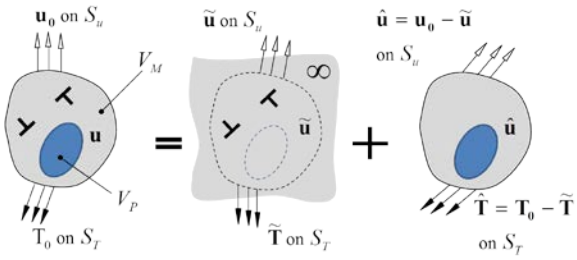

Figure 2: General discrete dislocation boundary value problem using the superposition scheme of Van der Giessen *et al*, 1995 [9].

The general discrete dislocation boundary value problem is shown in Figure 2 for an arbitrary body of volume V subject to boundary conditions $\mathbf{u}=\mathbf{u_0}$ on S_u, and $\mathbf{T}=\mathbf{T_0}$ on S_T. The body V is composed of an elastic-plastic matrix, V_M, and an elastic inclusion or particle, V_P, with elastic modulus L^M_{ijkl} and L^P_{ijkl}, respectively. The stress, strain and displacement fields are written as

$$\sigma_{ij} = \tilde{\sigma}_{ij} + \hat{\sigma}_{ij}, \quad \varepsilon_{ij} = \tilde{\varepsilon}_{ij} + \hat{\varepsilon}_{ij}, \quad u_{ij} = \tilde{u}_{ij} + \hat{u}_{ij} \tag{1}$$

where the (~)- fields are the singular fields associated with each individual dislocation in an infinite body of a homogeneous matrix material and the (^)-fields are the corrective fields for the actual boundary conditions, finite geometry and presence of inclusions.

The strain-displacement relations are related by

$$\varepsilon_{ij} = \frac{1}{2}\left(\frac{\partial u_i}{\partial x_j} + \frac{\partial u_j}{\partial x_i}\right) \tag{2}$$

The stress field satisfies the equilibrium equation

$$\frac{\partial \sigma_{ij}}{\partial x_j} = 0 \tag{3}$$

With V_M denoting the volume occupied by the matrix and V_P the volume occupied by the particle, the stress and strain fields are related by

$$\sigma_{ij} = \begin{cases} L^M_{ijkl}\varepsilon_{kl} & in\ V_M \\ L^P_{ijkl}\varepsilon_{kl} & in\ V_P \end{cases} \tag{4}$$

Throughout $V=V_M+V_P$, the dislocation stress field $\tilde{\sigma}_{ij}$ is related to the strain field $\tilde{\varepsilon}_{kl}$ by

$$\sigma_{ij} = L^M_{ijkl}\tilde{\varepsilon}_{kl} \tag{5}$$

Hence,

$$\hat{\sigma}_{ij} = \begin{cases} L^M_{ijkl}\hat{\varepsilon}_{kl} & in\ V_M \\ L^P_{ijkl}\hat{\varepsilon}_{kl} + (L^P_{ijkl} - L^M_{ijkl})\tilde{\varepsilon}_{kl} & in\ V_P \end{cases} \tag{6}$$

The polarization stress term, $(L^P_{ijkl} - L^M_{ijkl})\tilde{\varepsilon}_{kl}$ in Equation (6) vanishes for a homogeneous elastic material, i.e. for $L^P_{ijkl} \equiv L^M_{ijkl}$. Since $\tilde{\sigma}_{ij}$ satisfies equilibrium throughout V, $\hat{\sigma}_{ij}$ satisfies

$$\frac{\partial \hat{\sigma}_{ij}}{\partial x_j} = 0 \tag{7}$$

in V with the boundary conditions

$$\hat{u}_i = u_{0,i} - \tilde{u}_i \ on\ S_u, \quad \hat{T}_i = T_{0,i} - \tilde{T}_i \ on\ S_T \tag{8}$$

where S_u is that part of the boundary on which displacements $u_{0,i}$ are prescribed, and S_T that part of the boundary on which tractions $T_{0,i}$ are prescribed, with $T_i = \sigma_{ij} n_j$ and n_j is the outward normal to the surface. Equations (7) and (8) together with the constitutive relation Equation (6) give a boundary value problem for the (^)-fields.

The (^)-fields are smooth in V and a finite element method is used to obtain a solution. The polarization stress, $(L^P_{ijkl} - L^M_{ijkl})\tilde{\varepsilon}_{kl}$ in Equation (6) for V_P, is computed in FEM as a body force.

2.1.1 Dislocation constitutive rules

The 2d-DD method of Van der Giessen *et al*. [9] treats edge dislocations with Burgers vector b as line defects in a plane strain problem of elastically-isotropic single-crystal materials. The potentially active slip planes are introduced with a given spacing d. The evolution of dislocations is modeled through a set of constitutive rules governing dislocation glide, nucleation, annihilation and interaction with obstacles. Dislocation glide is controlled by Peach-Koehler force. The component of Peach-Koehler force on the slip plane and normal to the dislocation line is the driving force for dislocation glide, which for the I^{th} dislocation is

$$f^{(I)} = m_j\left(\hat{\sigma}_{ji} + \sum_{J\neq I}^{N_d}\sigma^{(J)}_{ji}\right)b_i \tag{9}$$

where b_i are the vector components of the Burgers vector on the slip planes, m_j are the components of the slip plane normal, σ_{ij} are the total stress tensor components at the location of the dislocation and N_d

is the number of dislocations. The total stress includes applied stress, image stresses, and the interaction stresses with all other dislocations. In most DD simulations the glide velocity υ is taken to be linearly related to the Peach-Koehler force *f* with a drag coefficient *B* written as

$$\upsilon^{(I)} = \frac{f^{(I)}}{B} \tag{10}$$

and dislocation positions are updated using a forward-Euler scheme. For FCC modeling, there are three slip systems initially free of dislocations, but dislocations can be generated from discrete Frank-Read-like sources that are randomly distributed on the slip planes with a density ρ_s. These sources generate dislocation dipoles when the Peach-Koehler force exceeds a critical value of $\tau_s b$ during a period of time t_{nuc}, with the sign of the dipole determined by the direction of Peach-Koehler force. The initial width of the generated dipole L_{nuc} is chosen so that the two dislocations are in equilibrium at the nucleation stress,

$$L_{nuc} = \frac{E}{4\pi(1-\nu^2)}\frac{b}{\tau_{nuc}} \tag{11}$$

where *E* is Young's Modulus and *v* is Poisson's ratio. Annihilation of two oppositely signed dislocations on the same slip plane occurs when they come within a critical distance of $L_e = 6b$ [43]. Obstacles blocking dislocation motion are also randomly placed on the slip planes to represent small precipitates, solutes, or forest dislocations. The obstacles pin the dislocations until the Peach-Koehler force is sufficient to overcome the obstacle strength τ_{obs}. It is worth noting that the DD method does ***not*** solve for equilibrium dislocation distributions. Since dislocations always have velocity which is proportional to Peach-Koehler force, the dislocation configuration at the end of any increment is an instantaneous snapshot of the constantly evolving dislocation structure.

2.1.2 An interface model for Mode-I crack growth

A common technique in the numerical modeling of fracture crack growth is that of the cohesive zone model. While a wide assortment of specific cohesive zone models have been used to model fracture in metals [44-46], the laws are in general defined by the maximum cohesive strength and a length scale. Measurement and first principle calculation (Quantum-based calculation) suggest that, for cleavage of atomic planes in crystalline metals, the peak traction is on the order of *gigapascals*, and the cohesive length is on the order of *nanometers*, giving a work of separation of roughly 1 J/m^2 for most metals [47]. However, for numerical implementation, such large cohesive strengths and small cohesive lengths demand an extremely fine mesh to resolve the stress gradients in the vicinity of the crack tip. By this way, the cohesive zone characterizes a fracture process over hundreds or thousands of atomic planes, rather than between two planes of atoms.

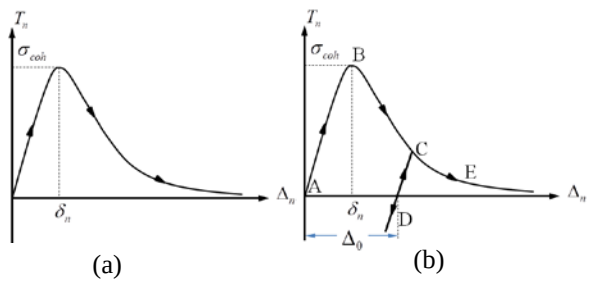

Figure 3: Schematics of cohesive zone laws (a) the reversibly cohesive relation (b) the irreversibly cohesive relation.

Here we focus on the fracture/fatigue problems Mode-I crack growth where the symmetry with respect to the crack plane is used, so only the upper half of the crystal is directly simulated. Crack growth is modeled using a cohesive zone model which extends along the crack plane. Along the cohesive surface, $T_1=0$ from symmetry while $T_2=T_n$ (in opening direction) has a universal binding form [48], as shown in Figure (3a). In the reversible case, the cohesive behavior for both loading and unloading behavior follows the same curve as

$$T_n(\Delta_n) = -\frac{\sigma_{coh}\Delta_n}{\delta_n}\exp\left(\frac{\delta_n - \Delta_n}{\delta_n}\right) \tag{12}$$

where $\Delta_n = 2u_2(x_1, x_2 = 0)$, σ_{coh} is the normal cohesive strength and δ_n is a characteristic opening length. A cohesive relation that accounts for the irreversibility of separation is modeled by specifying unloading from and reloading to the monotonic cohesive function, as illustrated in Figure (3b). Unloading from point C takes place along path CD, with stiffness

$$\frac{\partial T_n}{\partial \Delta_n} = -\frac{\exp(1)\sigma_{coh}}{\delta_n} \tag{13}$$

During the reloading, the traction increases along DC and then follows the original softening curve BCE. This is a phenomenological cohesive relation introduced to model the effects of irreversibility arising from the formation of an oxide layer [27]. Under continued cyclic loading conditions, the permanent opening Δ_0 (see Figure (3b)) grows, but only up to a value Δ_n=4 nm which is a representative value for the oxide layer thickness on aluminium under ambient conditions [49]. The work of separation is $\phi_n = \exp(1)\delta_n\sigma_{coh}$ corresponding to a Mode-I fracture toughness in the absence of plasticity which is given by

$$K_0 = \sqrt{\frac{E\phi_n}{1-\nu^2}} \tag{14}$$

In all calculations, a finite element mesh consisting of bilinear quadrilateral elements is employed. The length of the nonlinear cohesive region ahead of the crack tip, δ_c, just at the point of crack growth is

$$\delta_c = \frac{\pi\phi_n E}{8\sigma_{coh}^2} \tag{15}$$

This length is used to define the minimum mesh spacing of width $\delta_c/4$, which is used over a region that extends $40\delta_c$ ahead of the initial crack tip.

In the numerical solutions of the DD problem, extreme care, however, must be taken in the presence of the cohesive zone particularly when the cohesive zone lengths are comparable to atomistically-derived values.

2.2 *New algorithm and improvement*

As mentioned before, several modifications to the existing 2d-DD and cohesive zone methodology have been made by [41]. These modifications significantly improve the capability to model materials with the realistic material properties, especially cohesive properties. A brief overview of the new approach for improvements is presented in this section.

2.2.1 A new superposition technique

A new superposition scheme along with a Newton-Raphson iterative scheme was first suggested by [38]. The motivation of this new superposition framework is to reduce the computational cost in calculating polarization stress for elastically inhomogeneous problems. Also the new superposition framework is found to have several other important benefits: (i) the DD calculation is largely decoupled from the specific model geometry and boundary conditions and (ii) ability to easily model bodies with multiple distinct regions of dislocation activities, e.g. polycrystalline metal [50], metallic multi-layers [33, 51].

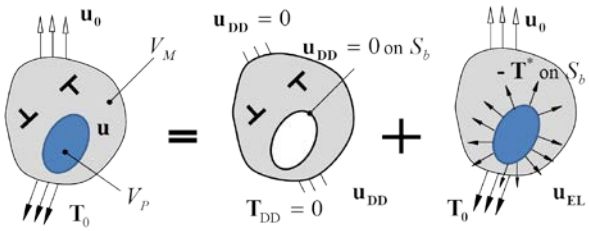

Figure 4: Schematic decomposition into two subsidiary problems: (DD) homogeneous discrete dislocation sub-problem solved with the standard formulation, subject to zero displacement boundary conditions and (EL) elastic sub-problem contain all specific boundary conditions and loading, solved with standard elastic FEM [38].

The decomposition of the new superposition scheme is illustrated in Figure 4. The total field is composed of (i) a homogeneous discrete dislocation sub-problem (DD) subject to zero displacement boundary conditions and (ii) a fully elastic sub-problem (EL) subject to all actual boundary conditions. The DD sub-problem is solved using the standard DD methodology but with the special boundary conditions while the EL sub-problem is solved using standard finite element methodology with a Newton-Raphson(NR) iterative scheme to capture accurately the nonlinearity of the interface (e.g. the cohesive zone interface and the particle/matrix interface, etc.). The DD sub-problem encompasses only the portion of the structure where dislocation activity is permitted. The key point is that the DD sub-problem is always homogeneous so that the polarization stresses vanish. An outcome of the DD sub-problem solution at each increment is a traction $\mathbf{T}^*$ along the constrained boundary S_b, thus information about the dislocation structure in any plastic regions of the body is transmitted to the remainder of the structure through the addition of a body force $-\mathbf{T}^*$ along S_b in EL sub-problem, as shown in Figure 4. [41] showed that various instabilities reported when using the standard superposition are eliminated with the use of this new superposition scheme.

2.2.2 A moving mesh scheme

The moving mesh method is implemented to capture micrometer crack growth with *nanometer* mesh sizes. The essence of this method is that, in a frame of reference moving with the crack tip, the dislocations and all field variables including those of cohesive zone can be considered as moving in the opposite direction. The moving mesh method allows the crack to grow forward for some distance and then shifts the dislocations and field variables backward by exactly that amount. This re-establishes the crack tip at the original location relative to the original mesh and leaves the stiffness matrix unchanged, Figure 5. A more detailed description is given in the work of [41].

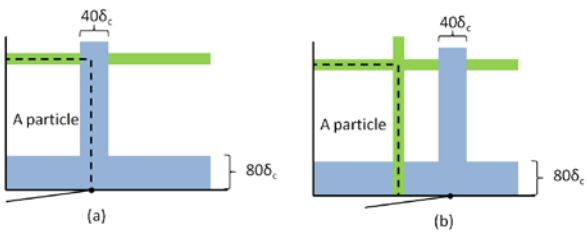

Figure 5: Schematic illustration of moving mesh for a cracked particle in the matrix problems with symmetric boundaries (a) the initial mesh where the crack tip is at the interface of a particle and the matrix (b) remeshing according to the current crack tip.

2.2.3 Velocity gradient correction

The gradient correction for computing dislocation velocity completely eliminates instabilities and oscillations in the standard forward-Euler approach.

The incremental dislocation motion gives rise to spurious large interaction forces when the dislocations become too close. To avoid unfavorable behavior, the gradient correction of the mobility law proposed by [41] is given as

$$\upsilon = \begin{cases} f - \tau_f b\, sign(f) \dfrac{1}{\left(1 - \dfrac{1}{B}\dfrac{\partial f}{\partial x}\Delta t\right)}; & if \ |f| > \tau_f b \\ 0 & ; otherwise \end{cases} \quad (16)$$

where B is a drag coefficient of dislocations on the slip planes and τ_f is a frictional stress on the slip planes. This correction also precludes the introduction of an artificially-low cut-off velocity for dislocation motion.

2.2.4 Modified dislocation nucleation

In generic DD simulations, a dislocation dipole is instantaneously nucleated at a distance $L_{nuc}/2$ on each side of the source when the stress on the source is greater than the source strength τ_{nuc} for a time period t_{nuc}. For the sources located close to the crack surface, the abrupt injection of a dislocation dipole results in a sudden jump in the displacement field on the crack boundary, which causes numerical instabilities. In addition, spurious forces are introduced on dislocation pileups due to the sudden injection of a dipole into the existing pileup.

To avoid large spurious forces arising from the abrupt introduction of a newly-nucleated dipole, the "latent" nucleating dislocations in the dipole are introduced gradually over the nucleation time t_{nuc} so that the Burger vector and the separation distance of the virtual dipole increase linearly with time as

$$b^{dipole}(t) = b\frac{t}{t_{nuc}}, \quad t < t_{nuc}, \quad \tau > \tau_{nuc} \quad (17)$$

$$x^{dipole}(t) = L_{nuc}\frac{t}{t_{nuc}}, \quad t < t_{nuc}, \quad \tau > \tau_{nuc} \quad (18)$$

Specifically, the *latent* dislocations are not subject to the mobility law until $t \geq t_{nuc}$, but do contribute to the Peach-Koehler forces on all other dislocations and to the displacements and traction on the boundaries [41].

3 Some discrete dislocation predictions

3.1 *Fatigue crack growth in multi-phase material*

A wide variety of structural alloys contain brittle particles dispersed in a ductile metallic matrix. While such particles are sometimes added for structural purposes, more often they arise during processing. These particles, or inclusions, are often undesirable by products of the material fabrication because fracture can originate by particle cracking followed by propagation into the surrounding ductile matrix. In particular, under cyclic loading conditions, cracks formed during processing or during the initial stages of loading will grow and ultimately lead to failure of the structure or component.

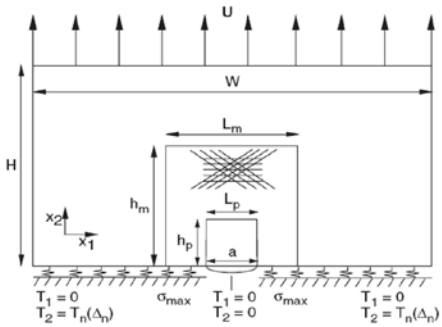

Figure 6: Sketch of analysed specimen for fatigue crack growth from a cracked particle with imposed boundary condition [34].

A planar single crystal (elastically isotropic with a Young's modulus E_m) reinforced by a 10 μm isotropic elastic particle (Young's modulus E_p) containing an initial crack was considered in [34]. The particle was taken to be completely cracked so that the initial crack length is equal to the particle size. Crack growth into the surrounding crystal was modeled via a cohesive framework. Initially, the three slip systems are free of mobile dislocations, but dislocations are nucleated from point sources, randomly distributed with a density of 20 per μm^2. There is a random distribution of 50 point obstacles per μm^2, which represent either small precipitates on the slip plane or forest dislocations on out-of-plane slip systems. These obstacles pin dislocations until the Peach-Koehler force attains the obstacle strength τ_{obs}, where τ_{obs} =60 MPa. For computational convenience, dislocation sources and obstacles are restricted to a process window of dimensions L_m x h_m around the cracked particle with L_m=50 mm and h_m=50 mm (see Figure 6). The presence of the elastic particle influences crack growth due to the effects of: (i) the modulus mismatch on the crack tip stress intensity;

(ii) this stress intensity on the evolution of plasticity; and (iii) the blocking of slip at the particle-matrix interface. These effects were investigated separately and sequentially by considering the three cases summarized in Table 1: (i) material A, an initially cracked single crystal, which should thus show only small crack effects; (ii) material B, a particle with the same elastic properties as the matrix, E_p=E_m but no dislocation activity inside the particle, which should show the effects of slip blocking only; and (iii) material C, a particle that is elastically stiffer than the matrix, E_p=5E_m,which should show the joint effects of modulus mismatch and slip blocking.

Table 1: The three materials analysed by [34] for a cracked elastic particle (p) in a plastically deforming matrix (m)

Material	E_p/E_m	Particle	Dislocation active
A	1	No	N/A
B	1	Yes	No
C	5	Yes	Yes

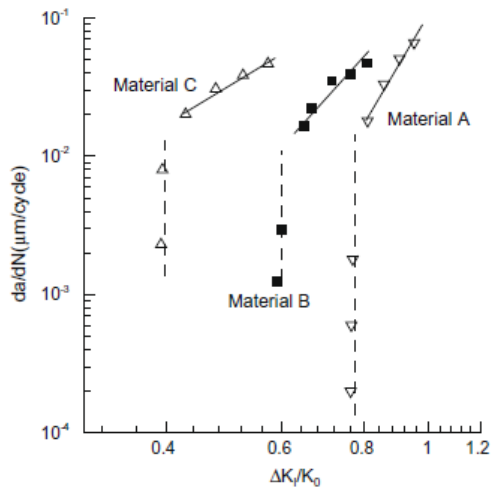

Figure 7: Discrete dislocation prediction of fatigue crack growth from a cracked particle [34].

Fatigue crack growth calculations for the three materials are shown in Figure 7. The calculations reveal a threshold for fatigue crack growth and a transition to a Paris law behavior, both depending on the existence of the elastic particle and the modulus mismatch. For a matched-modulus particle (Material B), the threshold is reduced by 25% relative to the single crystal (Material A) and this is attributed to slip blockage by the particle. For the high-modulus particle (Material C), the threshold is reduced by 50% relative to Material A and this is due to both slip blockage and the enhanced stress intensity factor due to the elastic mismatch. These results show that fatigue crack growth from micron-scale particles is strongly influenced by plasticity size effects, elastic mismatch, and particle constraints on plastic flow.

3.2 *Fracture for plastically anisotropic metals*

The intrinsic lattice resistance to dislocation motion, or Peierls stress, depends on the core structure of the dislocation and is one essential feature controlling plastic anisotropy in materials such as HCP Zn, Mg,

and Ti. The prior work on dislocation-based fracture modeling to include the effects of both Peierls stress and plastic anisotropy was extended to understand some evidences from the work on fracture of single crystal Zn by [52]. In that study, crack growth along the basal plane (easy-slip plane) was studied for two crack growth directions, $[2\bar{1}\,\bar{1}0]$ (orientation 1) and $[10\bar{1}0]$ (orientation 2) and complementary FEM crystal plasticity simulations were performed. Subsequently an anisotropic Peierls model as a friction stress was implemented within a 2d-DD plasticity model and the role of plastic anisotropy on the crack tip stress fields, crack growth, toughening, and microcracking were investigated [53]. In that work, tension tests (uncracked specimen), as shown in Figure 8, for a pure single crystal with no obstacles to dislocation motion were carried out to verify that the Peierls stress determines the yield stress in pure HCP-like materials having slip on basal and pyramidal planes. Then Mode-I crack growth in such a single crystal of the HCP material was analyzed using the modified 2d-DD model, Figure 9. Material properties are chosen to mimic HCP Zn with anisotropic slip properties listed in Table 2.

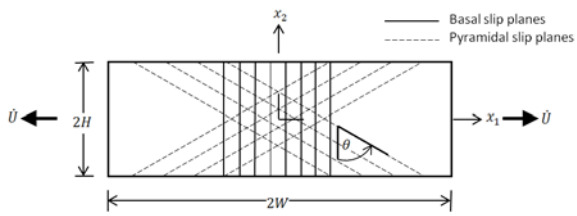

Figure 8: Geometry and boundary of tension problems [53].

The results show that the fracture toughness scales inversely with the tensile yield stress, largely independent of the plastic anisotropy, so that increasing Peierls stress on the pyramidal planes gives decreasing resistance to crack growth, consistent with recent experiments on Zn. Moreover, the DD simulations show that local stress concentrations, in Figure 10, exist sporadically along the pyramidal plane(s) that emanate from the current crack tip, suggesting an origin for experimentally-observed basal-plane microcracking near the tip of large cracks.

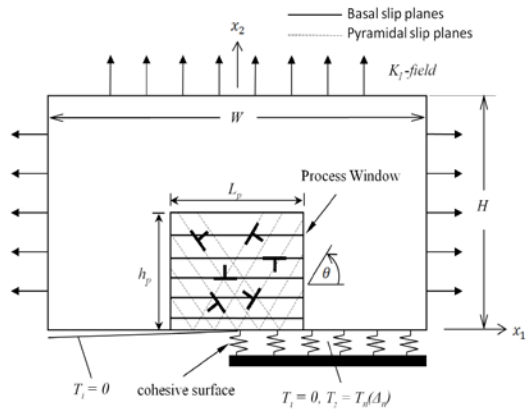

Figure 9: Schematic of the Mode-I crack problem with the imposed boundary conditions for plastically anisotropic metals [53].

Table 2: Anisotropic and isotropic properties of HCP-like materials studied

	τ_P^B (MPa)	τ_P^P (MPa)	b^B (nm)	b^P (nm)	B^B $\times 10^{-4}$(Pa.sec)	B^P $\times 10^{-4}$(Pa.sec)
Anisotropic	30	30	0.266	0.561	0.78235	2.10375
		60				
		90				
	60	60				
		120				
		180				
	90	90				
Isotropic	30		0.266		0.78235	
	60					
	90					

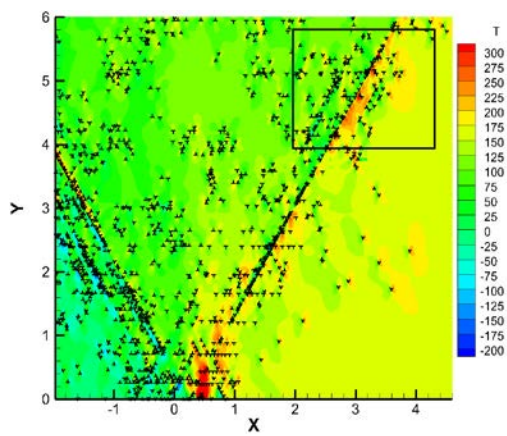

Figure 10: Total normal stress field over a large scale, showing local stress concentrations microns away from the crack tip [53].

Due to incomplete cancellation of dislocation stress fields in structure that are attempting to generate the constant stress sector expected from continuum-level analysis, [36-37], microcrack nucleation along basal plane may be a consequence of tensile stress concentration from the discreteness of the dislocation plasticity.

4 Modeling prospects

Modeling of fracture/fatigue via discrete dislocation plasticity provides a wide range of physical phenomena. In this 2d-DD, there is a variety of idealizations in the simulations of fracture/fatigue crack growth that need to be relaxed to obtain quantitatively useful predictions, for example;

- The analyses have been two dimensional, with both three-dimensional dislocation effects and three-dimensional crack growth effects neglected
- The effects of crack tip blunting are not taken into account in this small strain analysis
- The calculations have been carried out for small amounts of straight ahead crack growth in a single crystal, whereas experimental data typically are for larger amounts of crack growth in polycrystalline materials as a result in the microstructural aspects involved in crack transmission across a grain boundary [54]

Another modeling limitation is that this requires large amounts of computer time to enable calculations of larger amounts of crack growth and plastic zone (discrete dislocation zone). Additionally, fatigue crack growth rates are sensitive to the environment and accounting for environmental effects means accounting for chemistry in the crack tip region. This in turn requires an atomistic rather than a phenomenological cohesive model of the creation of new free surface. Using the multiscale modeling is a new direction for innovative research and can explore some of the above issues in fracture/fatigue mechanics. Multiscale modelling by coupling of a discrete dislocation region to a larger-scale continuum plasticity region for reducing computational cost and to a smaller-scale atomistic region around the crack tip for enhancing fidelity of the small-scale material description is thus one direction. In principal, all three scales, i.e. atomic, discrete dislocation, and continuum plasticity, can operate simultaneously within a single computational framework. Recently the success tool for the multiscale modeling with directly coupling the interface between different length scales are the coupled atomistic-discrete dislocation model (CADD) (e.g. [55-59]) and the coupled discrete dislocation-continuum plasticity [60]. Interestingly, the CADD framework is capable of incorporating a quantum mechanical description of the near tip, which is key for the accurate representation of chemistry, but at a significantly increased computational cost. At present, a full integration of methods has not been achieved but is ongoing research.

References

[1] Fleck, N. A., Muller, G. M., Ashby, M. F., & Hutchinson, J. W., 1994. Strain gradient plasticity: theory and experiment., *Acta Metallurgica et Materialia*, 42(2): 475-487.

[2] Gao, H., Huang, Y., Nix, W. D., & Hutchinson, J. W., 1999. Mechanism-based strain gradient plasticity-I. Theory., *Journal of the Mechanics and Physics of Solids*, 47(6): 1239-1263.

[3] Greer, J. R., Oliver, W. C., & Nix, W. D., 2005. Size dependence of mechanical properties of gold at the micron scale in the absence of strain gradients., *Acta Materialia*, 53(6): 1821-1830.

[4] Rice, J. R., 1971. Inelastic constitutive relations for solids: an internal-variable theory and its application to metal plasticity., *Journal of the Mechanics and Physics of Solids*, 19(6): 433-455.

[5] Anand, L., & Kothari, M., 1996. A computational procedure for rate-independent crystal plasticity., *Journal of the Mechanics and Physics of Solids*, 44(4): 525-558.

[6] Roters, F., Eisenlohr, P., Hantcherli, L., Tjahjanto, D. D., Bieler, T. R., & Raabe, D., 2010. Overview of constitutive laws, kinematics, homogenization and multiscale methods in crystal plasticity finite-element modeling: Theory, experiments, applications., *Acta Materialia*, 58(4): 1152-1211.

[7] Raabe, D., & Roters, F., 2004. Using texture components in crystal plasticity finite element simulations., *International Journal of Plasticity*, 20(3): 339-361.

[8] Raabe, D., & Becker, R. C., 2000. Coupling of a crystal plasticity finite-element model with a probabilistic cellular automaton for simulating primary static recrystallization in aluminium., *Modelling and Simulation in Materials Science and Engineering*, 8(4): 445.

[9] Van der Giessen, E., & Needleman, A., 1995. Discrete dislocation plasticity: a simple planar

model., *Modelling and Simulation in Materials Science and Engineering*, 3(5): 689.

[10] Cleveringa, H. H. M., Van der Giessen, E., & Needleman, A., 1997. Comparison of discrete dislocation and continuum plasticity predictions for a composite material., *ActaMaterialia*, 45(8): 3163-3179.

[11] Shu, J. Y., Fleck, N. A., Van der Giessen, E., & Needleman, A., 2001. Boundary layers in constrained plastic flow: comparison of nonlocal and discrete dislocation plasticity., *Journal of the Mechanics and Physics of Solids*, 49(6): 1361-1395.

[12] Cleveringa, H. H. M., Van der Giessen, E., & Needleman, A., 1999. A discrete dislocation analysis of bending., *International Journal of Plasticity*, 15(8): 837-868.

[13] Bulatov, V., & Cai, W., 2006. *Computer simulations of dislocations*, (Vol. 3). Oxford University Press.

[14] Arsenlis, A., Cai, W., Tang, M., Rhee, M., Oppelstrup, T., Hommes, G., & Bulatov, V. V., 2007. Enabling strain hardening simulations with dislocation dynamics., *Modelling and Simulation in Materials Science and Engineering*, 15(6): 553.

[15] Weinberger, C. R., Aubry, S., Lee, S. W., Nix, W. D., & Cai, W., 2009. Modelling dislocations in a free-standing thin film., *Modelling and Simulation in Materials Science and Engineering*, 17(7), 075007.

[16] Yasin, H., Zbib, H. M., & Khaleel, M. A., 2001. Size and boundary effects in discrete dislocation dynamics: coupling with continuum finite element., *Materials Science and Engineering: A*, 309: 294-299.

[17] Zbib, H. M., & Diaz de la Rubia, T., 2002. A multiscale model of plasticity., *International Journal of Plasticity*, 18(9): 1133-1163.

[18] Kohlhoff, S., Gumbsch, P., & Fischmeister, H. F., 1991. Crack propagation in bcc crystals studied with a combined finite-element and atomistic model., *Philosophical Magazine A*, 64(4): 851-878.

[19] Abraham, F. F., Schneider, D., Land, B., Lifka, D., Skovira, J., Gerner, J., & Rosenkrantz, M., 1997. Instability dynamics in three-dimensional fracture: an atomistic simulation., *Journal of the Mechanics and Physics of Solids*, 45(9): 1461-1471.

[20] Gao, H., Huang, Y., & Abraham, F. F., 2001. Continuum and atomistic studies of intersonic crack propagation. *Journal of the Mechanics and Physics of Solids*, 49(9): 2113-2132.

[21] Rountree, C. L., Kalia, R. K., Lidorikis, E., Nakano, A., Van Brutzel, L., & Vashishta, P., 2002. Atomistic aspects of crack propagation in brittle materials: Multimillion atom molecular dynamics simulations. *Annual Review of Materials Research*, 32(1): 377-400.

[22] Daw, M. S., & Baskes, M. I., 1984. Embedded-atom method: Derivation and application to impurities, surfaces, and other defects in metals., *Physical Review B*, 29(12): 6443.

[23] Foiles, S. M., Baskes, M. I., & Daw, M. S., 1986. Embedded-atom-method functions for the fcc metals Cu, Ag, Au, Ni, Pd, Pt, and their alloys., *Physical Review B*, 33(12): 7983.

[24] Daw, M. S., Foiles, S. M., & Baskes, M. I., 1993. The embedded-atom method: a review of theory and applications., *Materials Science Reports*, 9(7): 251-310.

[25] Cleveringa, H. H. M., Van der Giessen, E., & Needleman, A., 2000. A discrete dislocation analysis of mode I crack growth., *Journal of the Mechanics and Physics of Solids*, 48(6): 1133-1157.

[26] Van der Giessen, E., Deshpande, V. S., Cleveringa, H. H. M., & Needleman, A., 2001. Discrete dislocation plasticity and crack tip fields in single crystals., *Journal of the Mechanics and Physics of Solids*, 49(9): 2133-2153.

[27] Deshpande, V. S., Needleman, A., & Van der Giessen, E., 2001. A discrete dislocation analysis of near-threshold fatigue crack growth., *Acta materialia*, 49(16): 3189-3203.

[28] Deshpande, V. S., Needleman, A., & Van der Giessen, E., 2002. Discrete dislocation modeling of fatigue crack propagation., *Acta materialia*, 50(4): 831-846.

[29] Deshpande, V. S., Needleman, A., & Van der Giessen, E., 2003. Discrete dislocation plasticity modeling of short cracks in single crystals., *Acta Materialia*, 51(1): 1-15.

[30] Deshpande, V. S., Needleman, A., & Van der Giessen, E., 2003. Scaling of discrete dislocation predictions for near-threshold fatigue crack growth., *Acta Materialia*, 51(15), 4637-4651.

[31] Deshpande, V. S., Needleman, A., & Van der Giessen, E., 2003. Finite strain discrete dislocation plasticity., *Journal of the Mechanics and Physics of Solids*, 51(11): 2057-2083.

[32] Balint, D. S., Deshpande, V. S., Needleman, A., & Van der Giessen, E., 2005. Discrete dislocation plasticity analysis of crack-tip fields in polycrystalline materials., *Philosophical Magazine*, 85(26-27): 3047-3071.

[33] O'day, M. P., & Curtin, W. A., 2005. Bimaterial interface fracture: A discrete dislocation model., *Journal of the Mechanics and Physics of Solids*, 53(2): 359-382.

[34] Groh, S., Olarnrithinun, S., Curtin, W. A., Needleman, A., Deshpande, V. S., & Giessen, E. V. D., 2008. Fatigue crack growth from a cracked elastic particle into a ductile matrix., *Philosophical Magazine*, 88(30-32): 3565-3583.

[35] Bittencourt, E., Needleman, A., Gurtin, M. E., & Van der Giessen, E., 2003. A comparison of nonlocal continuum and discrete dislocation plasticity predictions., *Journal of the Mechanics and Physics of Solids*, 51(2): 281-310.

[36] Rice, J. R., 1987. Tensile crack tip fields in elastic-ideally plastic crystals., *Mechanics of Materials*, 6(4): 317-335.

[37] Drugan, W. J., Rice, J. R., & Sham, T. L., 1982. Asymptotic analysis of growing plane strain tensile cracks in elastic-ideally plastic solids., *Journal of the Mechanics and Physics of Solids*, 30(6): 447-473.

[38] O'day, M. P., & Curtin, W. A., 2004. A superposition framework for discrete dislocation plasticity. *Transactions of the ASME-E-Journal of Applied Mechanics*, 71(6): 805-815.

[39] Chakravarthy, S. S., & Curtin, W. A., 2010. Effect of source and obstacle strengths on yield stress: A discrete dislocation study., *Journal of the Mechanics and Physics of Solids*, 58(5): 625-635.

[40] Chakravarthy, S. S., & Curtin, W. A., 2010. Origin of plasticity length-scale effects in fracture., *Physical review letters*, 105(11), 115502.

[41] Chakravarthy, S. S., & Curtin, W. A., 2011. New algorithms for discrete dislocation modeling of fracture., *Modelling and Simulation in Materials Science and Engineering*, 19(4), 045009.

[42] Hull, D., & Bacon, D. J., 2011., *Introduction to dislocations* (Vol. 37). Access Online via Elsevier.

[43] Bréchet, Y., Kubin, L. P., Devincre, B., Condat, M., Pontikis, V., & Canova, G., 1992. Dislocation microstructures and plastic flow: a 3D simulation., *Solid State Phenomena*, 23: 455-472.

[44] Needleman, A., 1987. A continuum model for void nucleation by inclusion debonding., *Journal of applied mechanics*, 54(3): 525-531.

[45] Xu, X. P., & Needleman, A., 1994. Numerical simulations of fast crack growth in brittle solids., *Journal of the Mechanics and Physics of Solids*, 42(9): 1397-1434.

[46] Tvergaard, V., & Hutchinson, J. W., 1996. Effect of strain-dependent cohesive zone model on predictions of crack growth resistance., *International Journal of Solids and Structures*, 33(20): 3297-3308.

[47] Raynolds, J. E., Smith, J. R., Zhao, G. L., & Srolovitz, D. J., 1996. Adhesion in NiAl-Cr from first principles., *Physical Review B*, 53(20), 13883.

[48] Rose, J. H., Ferrante, J., & Smith, J. R., 1981. Universal binding energy curves for metals and bimetallic interfaces., *Physical Review Letters*, 47: 675-678.

[49] Do, T., McIntyre, N. S., Van der Heide, P. A. W., & Akano, U. G., 1999. Oxidation kinetics of Mg-, Si-, and Fe-implanted aluminum by using X-ray photoelectron spectroscopy., *The Journal of Physical Chemistry B*, 103(13): 2402-2407.

[50] Shishvan, S. S., Mohammadi, S., Rahimian, M., & Van der Giessen, E., 2011. Plane-strain discrete dislocation plasticity incorporating anisotropic elasticity., *International Journal of Solids and Structures*, 48(2): 374-387.

[51] Chng, A. C., O'Day, M. P., Curtin, W. A., Tay, A. A., & Lim, K. M., 2006. Fracture in confined thin films: a discrete dislocation study., *Acta materialia*, 54(4): 1017-1027.

[52] Catoor, D., & Kumar, K. S., 2008. Crack growth on the basal plane in single crystal zinc: experiments and computations., *Philosophical Magazine*, 88(10): 1437-1460.

[53] Olarnrithinun, S., Chakravarthy, S. S., & Curtin, W. A., 2013. Discrete dislocation modeling of fracture in plastically anisotropic metals., *Journal of the Mechanics and Physics of Solids*.

[54] Catoor, D., & Kumar, K. S., 2011. Crack–grain boundary interactions in zinc bicrystals., *Philosophical Magazine*, 91(16): 2154-2185.

[55] Shilkrot, L. E., Miller, R. E., & Curtin, W. A., 2002. Coupled atomistic and discrete dislocation plasticity., *Physical review letters*, 89(2): 025501.

[56] Curtin, W. A., & Miller, R. E., 2003. Atomistic/continuum coupling in computational materials science., *Modelling and simulation in materials science and engineering*, 11(3), R33.

[57] Xiao, S. P., & Belytschko, T., 2004. A bridging domain method for coupling continua with molecular dynamics., *Computer methods in applied mechanics and engineering*, 193(17): 1645-1669.

[58] Warner, D. H., Curtin, W. A., & Qu, S., 2007. Rate dependence of crack-tip processes predicts twinning trends in fcc metals., *Nature Materials*, 6(11): 876-881.

[59] Song, J., & Curtin, W. A., 2011. A nanoscale mechanism of hydrogen embrittlement in metals., *Acta Materialia*, 59(4): 1557-1569.

[60] Wallin, M., Curtin, W. A., Ristinmaa, M., & Needleman, A., 2008. Multi-scale plasticity modeling: Coupled discrete dislocation and continuum crystal plasticity., *Journal of the Mechanics and Physics of Solids*, 56(11): 3167-3180.